Chinese Journal of
POLYMER SCIENCE

ARTICLE

https://doi.org/10.1007/s10118-020-2383-0
Chinese J. Polym. Sci. **2020**, *38*, 806–813

An Azoester-containing Photoresponsive Linear Liquid Crystal Polymer with Good Mesophase Stability

Shu-Qiang Han, Ying-Ying Chen, Bo Xu, Jia Wei*, and Yan-Lei Yu

Department of Materials Science and State Key Laboratory of Molecular Engineering of Polymers, Fudan University, Shanghai 200433, China

Electronic Supplementary Information

Abstract Photoresponsive linear liquid crystal polymers (LLCPs) are attractive because of the excellent stimuli-responsibility and the good processability. In this study, a new photoresponsive LLCP containing azoester (PC11AE6) with good mesophase stability was synthesized by ring-opening metathesis polymerization. By introducing photoresponsive azoester mesogenic unit, which has high rigidity and a large length-diameter ratio, the resultant polymer possesses a broad mesophase temperature interval (isotropic temperature = 180 °C). A study on mesophase by 2D-wide angle X-ray diffraction indicated that the mesogens were orientated spontaneously into smectic A phase after annealing. The orientated films and fibres exhibited macroscopic, rapid and reversible deformations under light irradiation as a result of the photoisomerization of azoester as confirmed by UV-Vis absorption spectrophotometry. We anticipate that this work provides a strategy for preparing LLCP with a broad mesophase temperature range, which is positive for potential applications.

Keywords Ring-opening metathesis polymerization; Liquid crystal polymers; Azoester; Photodeformation

Citation: Han, S. Q.; Chen, Y. Y.; Xu, B.; Wei, J.; Yu, Y. L. An azoester-containing photoresponsive linear liquid crystal polymer with good mesophase stability. *Chinese J. Polym. Sci.* **2020**, *38*, 806–813.

INTRODUCTION

Photodeformable polymers have received increasing attention in virtue of their potential in various applications such as artificial muscles, smart robots and locomotion systems.[1,2] Current efforts have been concentrated on the development of photodeformable liquid crystal polymers (LCPs)[3–6] due to their unique advantages endowed by liquid crystal molecules, such as self-organization, reversible phase transition and macroscopic orientation.[7] These properties allow the material to produce large and fast photoinduced mechanical responses when photosensitive chromophores are incorporated into LCPs. As important photoresponsive chromophores, azobenzene (azo) groups provide azo-functionalized LCPs with photoresponsive properties and bring a reversible shape change upon exposure to UV or visible light because of the reversible *trans-cis* photoisomerization.[8,9]

The azo-containing LCPs have been mostly prepared *via* free radical polymerization with chemical crosslink, which limits their application for fabricating complex devices due to the incompatibility with existing industrial processing methods. In order to break through this limitation, we designed azo-containing linear LCPs (LLCPs) with excellent mechanical properties endowed by high molecular weight through ring-opening metathesis polymerization (ROMP).[10–12] Owing to the linear structure, traditional melting and solution processing methods were applicable in the processing procedure of LLCPs, which was unattainable for the cross-linked LCPs. Furthermore, without the need for external orientation treatments (rubbing,[13–15] electric field,[16] magnetic field,[17,18] and others), an annealing treatment was enough to endow LLCPs with a highly ordered structure by the aid of flexible main chain and spacer.[19] These remarkable properties make these LLCPs excellent candidates for many applications, which inspires us to develop a homologous series with different molecular structures to satisfy different purposes. Their chemical and physical properties can be varied by introducing azo-derivatives, which act as both the mesogenic and photoresponsive units and have significant influence on the phase transition and photoresponsive behaviors.[20,21]

Photo-deformation of azo-containing LCP is normally derived from the photoinduced reversible phase transition between the ordered mesophase and the isotropic phase within the temperature range of mesophase. Therefore, it is important to widen mesophase temperature range for LLCPs to realize reliable photoresponsive properties in a broad temperature range. Azoester consisting of ester (—COO—)-azo (—N=N—) linkages is a useful group existing in liquid crystal molecules,[22] which is applicable for thermographic devices, optical imaging, and light emitting diodes.[23] When the phenyl is coupled with ester-azo linkage, the obtained

* Corresponding author, E-mail: weijia@fudan.edu.cn

Received November 1, 2019; Accepted December 28, 2019; Published online February 27, 2020

azoester is rigid and has a large length-diameter ratio. Compared with azo, the corresponding melting temperature and isotropic temperature of azoester increased accompanied by the widening of mesophase temperature range, which indicated the good phase stability of the compounds.[24,25] Thus, the azoester is an ideal mesogen for preparing phase stable photodeformable LLCPs to enrich the diversity of LLCPs and enlarge their application field.

In this study, azoester was introduced into LLCP to improve the phase stability attributed to the broad mesophase temperature range. The mesomorphism and thermal behaviors were investigated by polarizing optical microscopy (POM) and differential scanning calorimetry (DSC). The spontaneous orientation and photoresponsive behaviors of the LLCP were also studied. Moreover, the relationship between photodeformable behaviors and influencing factors, such as UV light intensity, film thickness and temperature, was investigated in detail.

EXPERIMENTAL

General Considerations

All chemical reagents required for preparation were used as received. Solvents were dried and distilled prior to use. ^{1}H-NMR spectra of PC11AE6 were recorded on a Bruker DMX500 NMR spectrometer using tetramethylsilane as the internal standard and chloroform-d as solvent. High resolution mass spectra (HR-MS) data were obtained by using electron spray ionization (ESI) Agilent 7250. The molecular weight of PC11AE6 and its polydispersity index were measured by gel permeation chromatography (GPC, Waters E2695) using tetrahydrofuran as the mobile phase. The thermodynamic properties of liquid crystal polymer PC11AE6 were determined by DSC (TA, Q2000) at a heating and cooling rate of 10 °C·min^{-1}. At least three scans were conducted to determine the reproducibility, and the third scan data were adopted. The mesomorphic property and phase transition behaviors of polymer were characterized with a polarizing optical microscope (POM, Leika, DM2500p) equipped with a hot stage (Linkam THMS600). Two dimensional-wide angle X-ray diffraction (2D-WAXD) experiments of PC11AE6 films and fibres were conducted on a small angle/wide angle scatterometer (Xeuss 2.0) with a 2D detector of Pilatus3R in transmission mode. The photoisomerization of azoester in the dichloromethane (CH_2Cl_2) solution of PC11AE6 was investigated by a UV-Vis spectrophotometer (Perkin Elmer, Lambda 650). The bending behaviors of films and fibres were recorded by an ultradepth 3D microscope (Keyence, VHX-1000C). 365 nm UV-light was generated by an Omron ZUV-H30MC light source with a ZUV-C30H controller. 530 nm visible light was generated by a CCS HLV-24GR-3W. The infrared images were captured by Infrared Thermal Camera (FLIR-E64501).

Synthesis of Monomer and PC11AE6

Synthesis of 4'-(11-hydroxyundecyloxy) hexyloxyphenyl azobenzoate (C)

Compounds A and B Scheme 1 were prepared according to the method reported previously.[24,26] The HCl and NaOH aqueous solutions in distilled water were added to adjust the pH of the reaction system. The yields of A and B were 63.33% and 60.76%, respectively. A mixture of B (3 g, 7.3 mmol), 4-(hexyloxy) phenol (2.1 g, 10 mmol) and 4-dimethylaminopyridine (DMAP, 0.89 g, 7.3 mmol) was stirred in 500 mL of CH_2Cl_2 under argon. The solution of 1-(3-dimethylaminopropyl)-3-ethylcarbodiimide hydrochloride (EDC, 2.87 g, 15 mmol) in CH_2Cl_2 (20 mL) was then added dropwise into the reaction mixture at room temperature. After stirring for 48 h, the precipitate formed during the reaction was filtered off and the solvent was evaporated to obtain a crude product. Then, the crude product was purified by silica gel column chromatography using CH_2Cl_2 as eluent. Vacuum-rotary evaporation procedure was necessary to obtain the product (3.1 g, 5.27 mmol, 72.2%). ^{1}H-NMR (500 MHz, chloroform-d, δ, ppm): 8.32 (d, J = 11 Hz, 2H), 7.96 (d, J = 11 Hz, 4H), 7.14 (d, J = 11.5 Hz, 2H), 7.03 (d, J = 11.5 Hz, 2H), 6.94 (d, J = 11.5 Hz, 2H), 4.06 (t, J = 16.5 Hz, 2H), 3.97 (t, J = 11.5 Hz, 2H), 3.65 (t, J = 11.5 Hz, 2H), 1.87–1.76 (m, 4H), 1.61–1.54 (m, 2H), 1.51–1.44 (m, 6H), 1.38–1.31 (m, 14H), 0.92 (t, J = 17.5 Hz, 3H).

Synthesis of monomer C11AE6

5-Succinate-1-cyclooctene (D) was synthesized according to a literature.[27] Intermediately, C (1.18 g, 2 mmol), D (0.54 g, 2.4 mmol) and DMAP (0.25 g, 2 mmol) were added into 200 mL of CH_2Cl_2. The solution of EDC (0.77 g, 4 mmol) in CH_2Cl_2 (20 mL) was then added dropwise into the reaction mixture at room temperature. After the mixture was stirred at room temperature under argon for 48 h, the crude product was purified by silica gel column chromatography using CH_2Cl_2 as the eluent. The vacuum-rotary evaporation and recrystallization procedures were necessary to obtain product (3.1 g, 5.27 mmol, 72.2%). The yield of monomer C11AE6 was 53%. ^{1}H-NMR (500 MHz, chloroform-d, δ, ppm): 8.32 (d, J = 8.5 Hz, 2H), 7.96 (d, J = 8.5 Hz, 4H), 7.14 (d, J = 9 Hz, 2H), 7.02 (d, J = 8.5 Hz, 2H), 6.94 (d, J = 9 Hz, 2H), 5.67–5.59 (m, 2H), 4.88–4.83 (m, 1H), 4.10–4.05 (m, 4H), 3.97 (t, J = 13 Hz, 2H), 2.62–2.56 (m, 4H), 2.16 (m, 4H), 1.92–1.77 (m, 6H), 1.66–1.59 (m, 4H), 1.52–1.45 (m, 4H), 1.40–1.28 (m, 16H), 0.92 (t, J = 14 Hz, 3H). HR-MS (m/z) $[M+H]^+$ Calcd. for $C_{48}H_{64}O_8N_2$, 797.4736; Found, 797.47008.

Synthesis of PC11AE6

The polymerization of monomer C11AE6 was performed by ROMP. C11AE6 (400 mg, 0.5 mmol) in distilled CH_2Cl_2 (1 mL) was placed into a Schlenk flask (25 mL). After the solution was degassed by freeze-pump-thaw cycles for three times, second generation Grubbs catalyst (0.8 mg) in 1 mL of degassed CH_2Cl_2 was injected into the Schlenk flask by syringe under argon. The mixture was stirred at 48 °C for 2 h. Upon vitrification, the reaction was terminated using ethyl vinyl ether, and a small amount of CH_2Cl_2 (~2 mL) was added to improve stirring. The contents were then precipitated into cold methanol, filtered, and dried under vacuum to yield the PC11AE6 (324 mg, 81%). M_n(GPC) = 3.0 × 10^5 g·mol^{-1}, M_w/M_n(GPC) = 1.50. ^{1}H-NMR (500 MHz, chloroform-d, δ, ppm): 8.32 (d, J = 8.5 Hz, 2H), 7.96 (d, J = 8.5 Hz, 4H), 7.14 (d, J = 9 Hz, 2H), 7.02 (d, J = 8.5 Hz, 2H), 6.94 (d, J = 9 Hz, 2H), 5.35 (m, 2H), 4.88–4.83 (m, 1H), 4.10–4.05 (m, 4H), 3.97 (t, J = 13 Hz, 2H), 2.62–2.56 (m, 4H), 2.16 (m, 4H), 1.92–1.77 (m, 6H), 1.66–1.59 (m, 4H), 1.52–1.45 (m, 4H), 1.40–1.28 (m, 16H), 0.92 (t, J = 14 Hz, 3H).

Preparation of PC11AE6 Films and Fibres

The thin films were prepared by the drop-coating method using a CH_2Cl_2 solution of PC11AE6 (3 wt% or 5 wt%) which was cast onto the dry and clean glass substrates. After solvent evapora-

https://doi.org/10.1007/s10118-020-2383-0

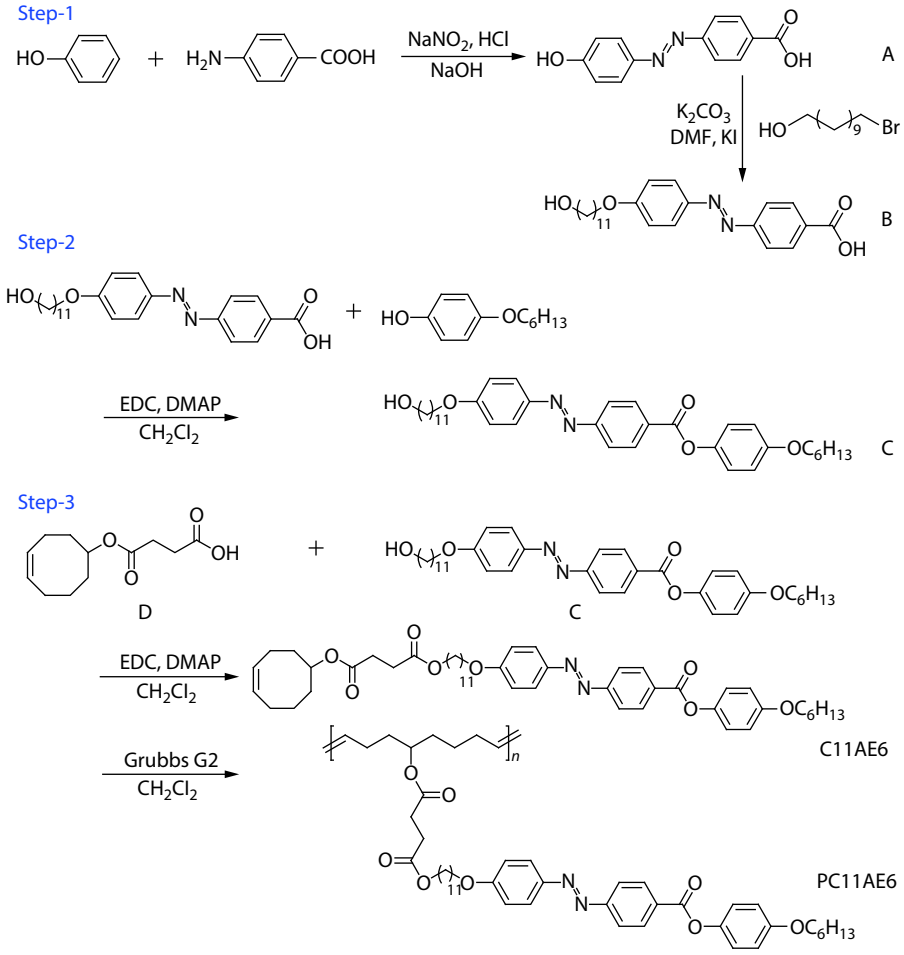

Scheme 1 Synthesis routes to PC11AE6.

ted, films were obtained by peeling them off from the substrates. The fibres were drawn from polymer melt in its isotropic state. A small amount of PC11AE6 was heated to 200 °C on a glass substrate placed on a hot stage. Then the fibres were drawn by using a toothpick to pull out quickly. An annealing process at 55 °C (3 h) was essential to obtain spontaneously oriented mesogens in PC11AE6 films and fibres before using.

RESULTS AND DISCUSSION

Synthesis and Characterization of PC11AE6

The azoester-containing LLCP (PC11AE6) was prepared as shown in Scheme 1. The ^{1}H-NMR spectrum of obtained polymer is shown in Fig. 1. The characteristic aromatic proton signals from 6.93 ppm to 8.31 ppm were observable and proportionable, which indicated the presence of azoester rigid unit. The presence of resonance signal around 5.35 ppm corresponding to the double-bond protons "g" from the main chain indicated the accomplishment of polymerization, with the absence of resonance signal at 5.6 ppm, which corresponded to the double-bond protons from cyclooctene of monomer C11AE6. The resonance signal area ratio of "*a*/*h* = 2" (7.01 and 4.87 ppm) was consistent with theory, which demonstrated the completed conjunction between main chain and side

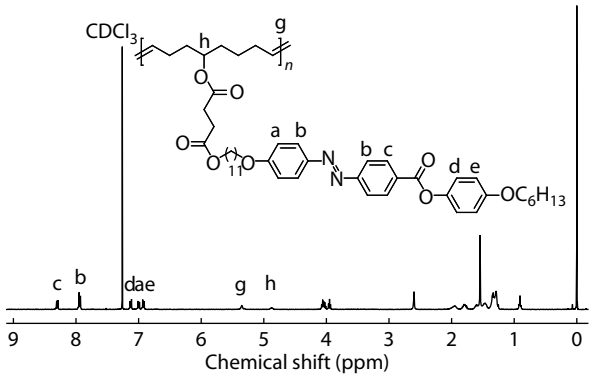

Fig. 1 ^{1}H-NMR spectrum of linear liquid crystal polymer PC11AE6.

chain. The molecular weight of obtained polymer was 3.0 × 10^5 g·mol^{-1}, which was one order of magnitude larger than that of the azo-containing methacrylate polymers obtained by conventional free radical polymerization.[21] With enhanced mechanical robustness endowed by high molecular weight, free-standing multidimensional shapes of PC11AE6, as shown in Fig. S1 (in the electronic supplementary information, ESI), were prepared by different processes, which satisfied different requirements in many application fields.

https://doi.org/10.1007/s10118-020-2383-0

Photochemical Isomerization of PC11AE6

The photoisomerization of azoester chromophore is at the origin of the attractive properties of polymers containing azoester mesogens. As shown in Fig. 2(a), upon firstly irradiation with 365 nm UV light (10 mW·cm^{-2}), PC11AE6 in CH_2Cl_2 solvent underwent *trans-cis* isomerization. As time went on, the intensity of the $\pi\rightarrow\pi^*$ transition band around 363 nm decreased, while the intensity of the $n\rightarrow\pi^*$ transition around 453 nm increased slightly. This procedure took 10 s until a photostationary state was eventually achieved. The existence of isobestic points is a strong evidence of the presence of two distinct absorbing bands in equilibrium with each other, and indicates that no side reaction occurs during the photoisomerization process.[28] As shown in Fig. 2(b), the *cis-trans* back isomerization was achieved through irradiating with visible light for 36 s. The reduction of content of the thermodynamically less stable *cis* form was confirmed by the intensity increase of the $\pi\rightarrow\pi^*$ transition band around 363 nm and the intensity decrease of the $n\rightarrow\pi^*$ transition around 453 nm. These results suggest that the azoester in polymer is able to undergo the photoisomerization in response to UV and visible light.

The Mesomorphic and Thermodynamic Properties of PC11AE6

As shown in Fig. 3(a), because of the linear structure and flexible main chain, PC11AE6 had a lower glass transition temperature (T_g = 48 °C). The polymer PC11AE6 possessed mesophase transition at 83 °C and reached isotropic state at about 182 °C. The POM results indicated the existence of birefringence as temperature decreased to 25 °C (Fig. 3b). Thus, the mesophase temperature interval of PC11AE6 was at least from 25 °C to 182 °C, which was wider than that of previously reported LLCP with azo in the side chains.[11] The temperature-varied 1D-WAXD data are shown in Fig. 3(c) and Fig. S2 (in ESI). In the low-angle region, two couples of diffraction peaks existed in 1D-WAXD curves (marked as $2\theta_1$ and $2\theta_2$ from 80 °C to 160 °C, $2\theta_3$ and $2\theta_4$ from 20 °C to 80 °C), with a ratio of scattering vector q ($q = 4\pi\sin\theta/\lambda$, with λ the X-ray wavelength and 2θ the scattering angle) of 1:2. This result indicates PC11AE6 formed two types of long-range ordered lamellar structures at different temperature ranges, with a d-spacing of ~4.60 nm ($2\theta_1$ = 1.92°) and ~5.04 nm ($2\theta_3$ = 1.75°) at high and low temperature, respectively.[29] In the high-angle region, the scattering halo with the maximum at $2\theta_5$ of ~20.5° was more diffusive when the temperature was above the phase transition temperature (about 80 °C), suggesting the molecular packing was less ordered at high temperature.

The Spontaneous Orientation of PC11AE6

The preferential orientation of mesogens is of vital importance for LCPs to deform in the anisotropic manner under external stimuli.[30–32] The spontaneous orientation of the LCPs should be the consequence of molecular cooperative effect of the rigid azoester mesogens. The flexible backbones and long spacers increase the molecular flexibility which facilitate the azoester mesogens to generate a highly ordered structure.[11] To determine the spontaneous orientation in PC11AE6, 2D-WAXD characterization was used. As investigated in Figs. 4(a) and 4(b), the split diffractions in the low- and high-angle regions demonstrated spontaneous formation of uniform mesogen orientation. Besides, the orientation of mesogens in fibre was

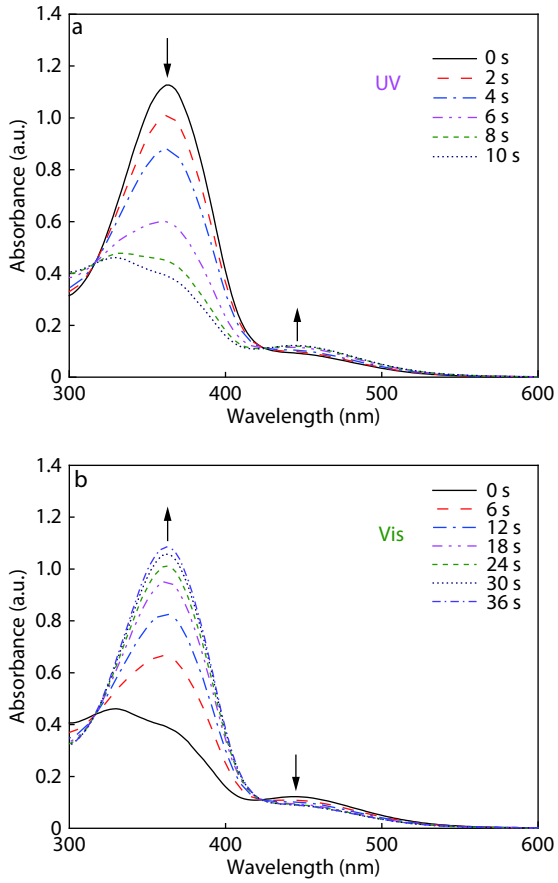

Fig. 2 The UV-Vis absorption spectra of PC11AE6 in CH_2Cl_2 solvent (c = 1.2 × 10^{-5} mol·L^{-1}) upon UV or visible light irradiation. UV-Vis absorption spectral changes in dependence of time for PC11AE6 at 25 °C (a) with irradiation of 365 nm UV light (power density = 10 mW·cm^{-2}) and (b) with irradiation of 530 nm visible light (power density = 30 mW·cm^{-2}).

similar to that of film. The diffraction arcs in the low-angle region appeared on the equator line in Figs. 4(a) and 4(b), implying the formation of the smectic phase with normal directions of the smectic layer perpendicular to the fibre axial direction or the film plane. In the high-angle region, two diffraction arcs on the meridian demonstrated the smectic A phase with out-of-plane orientation of the mesogens. Orientation parameter of fibre (S = 0.65) measured by WAXD was larger than that of film (S = 0.57), which may result from induced orientation produced by main chain extending process under fibre drawing. The schematic diagram of mesogen orientation both in PC11AE6 fibre and film is shown in Fig. 4(c). Out-of-plane orientation of mesogens was maintained in radial direction for fibre or thickness direction for film. Furthermore, when it exceeded the phase transition temperature, the mesophase changed from smectic A to smectic C with a tilting angle of 53°, which remained out-of-plane orientation of mesogens (Figs. S3 and S4 in ESI). The zigzag tilting of mesogens was generated in the lamella of smectic C. These results indicate that the anisotropic structures in the PC11AE6 fibre and film were formed, which established an important foundation for their photoresponsive deformation.

https://doi.org/10.1007/s10118-020-2383-0

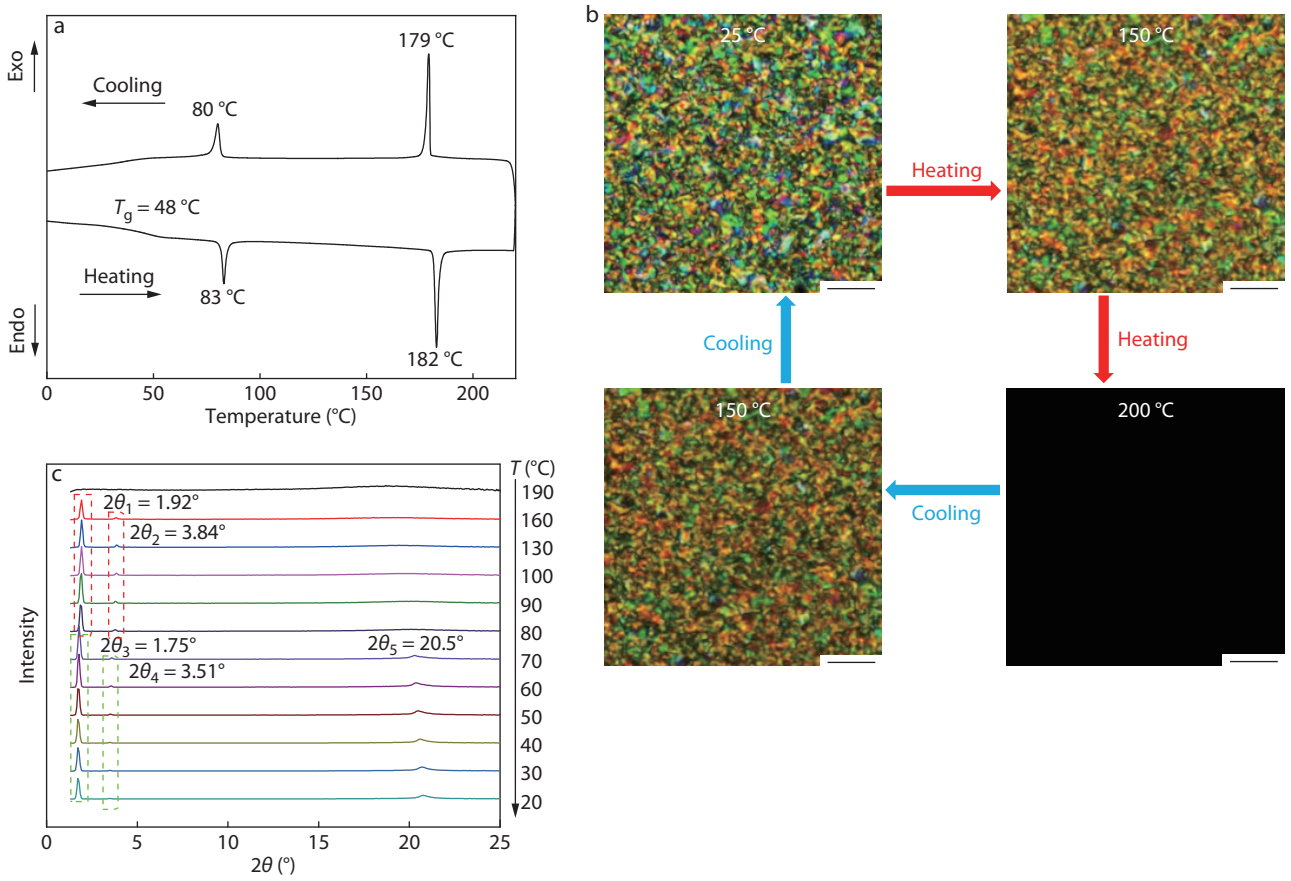

Fig. 3 Characterization of the mesomorphic properties and phase structure of linear liquid crystal polymer PC11AE6. (a) The DSC curves of PC11AE6 from the third heating scan and the third cooling scan (10 °C·min^{-1}). (b) The POM photographs of mesogenic phase transitions of PC11AE6 from the third heating and cooling cycle (10 °C·min^{-1}). The scale bar is 10 μm. (c) The 1D-WAXD patterns of PC11AE6 fibres detected in cooling process.

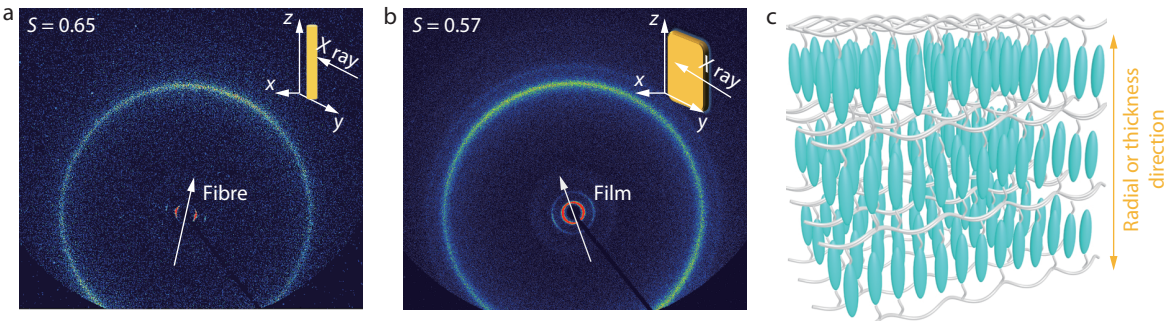

Fig. 4 Spontaneous orientation of PC11AE6 fibre and film. 2D-WAXD patterns and inserted orientation parameter values of PC11AE6 (a) fibre and (b) film. The X-ray beam was applied to the side of the materials and parallel to the axial direction of the fibre or the plane of the film. (c) Schematic diagram showing the liquid crystal orientation both in PC11AE6 fibre and film.

Photoinduced Reversible Deformation of PC11AE6

With the anisotropic structure, photoresponsive azoester-containing PC11AE6 exhibited reversible macroscopic deformation under illumination (Fig. 5). As shown in Fig. 5(a), upon UV irradiation (365 nm, 40 mW·cm^{-2}), the PC11AE6 films and fibres bent away from the light source to reach different bending angles. Thanks to the out-of-plane orientation of mesogens, the *trans-cis* photoisomerization caused the expansion on materials surfaces of PC11AE6, which led to the bending behaviors (Fig. 5a and Movies S1 and S2 in ESI).[33] The photoresponsibility of films with different thicknesses was investigated, as shown in Fig. 5(a) and Fig. S5 (in ESI). It should be noted that the bending angle of the thinner film (10 μm, 68°) was larger than that of the thicker one (20 μm, 21°). This is probably because that *trans-cis* photoisomerization reactions of azoester occurred only at the surface region of the films due to the large extinction coefficient of azoester moieties at about 360 nm when the PC11AE6 films were irradiated with UV light

https://doi.org/10.1007/s10118-020-2383-0

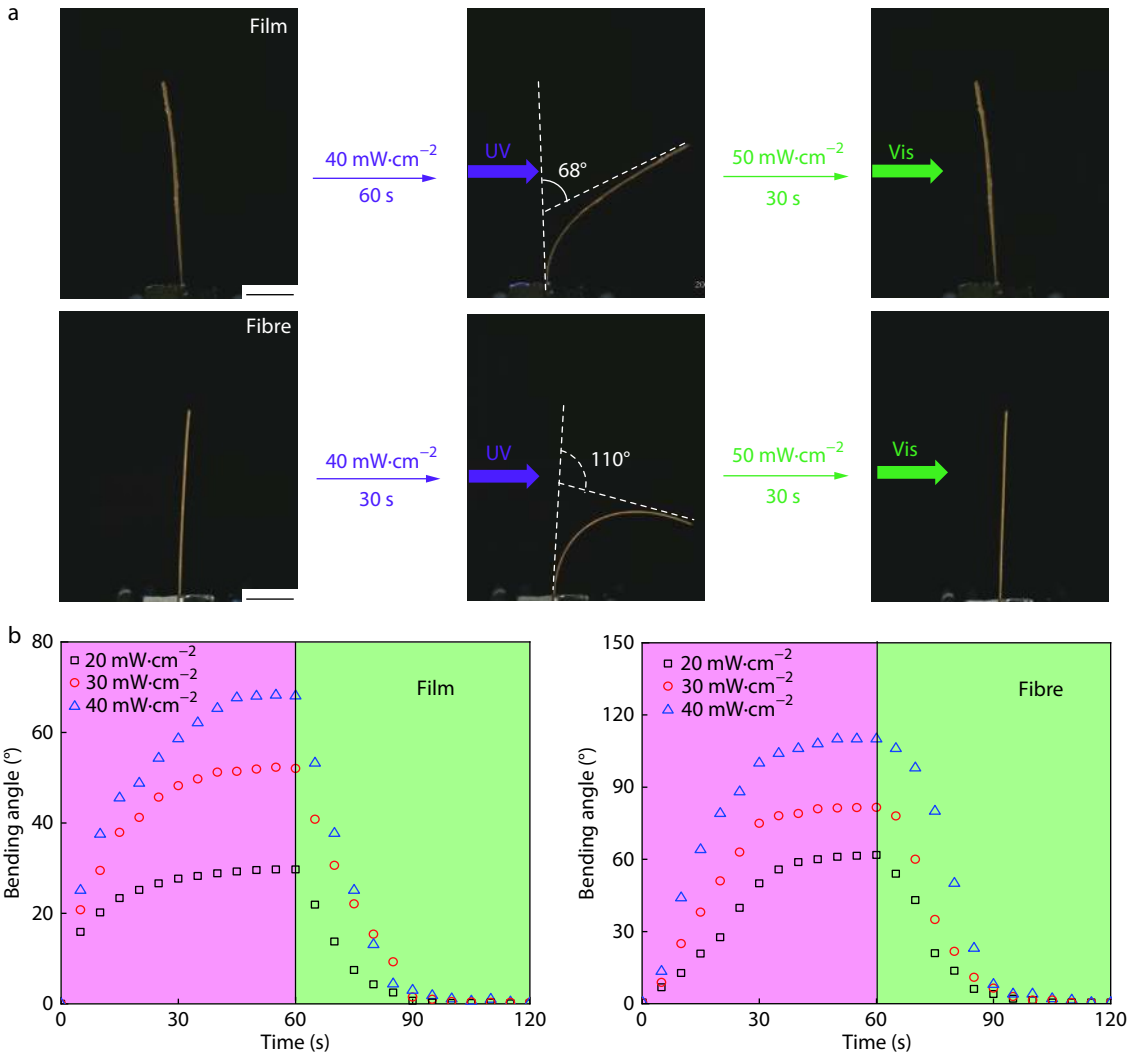

Fig. 5 The reversible photo-induced deformation behaviors of PC11AE6 films and fibres upon irradiation with 365 nm UV light and 530 nm visible light at room temperature. (a) The photodeformation of films and fibres upon irradiation from left. The size of films used here is 5 mm × 1 mm × 10 μm, while the diameter for fibres is 40 μm. The scale bar is 1 mm. (b) The relationship between bending angle and irradiation time of PC11AE6 films (10 μm) and fibres (40 μm) upon UV irradiation with different intensities. The visible light intensity was always kept at 50 mW·cm^{-2}.

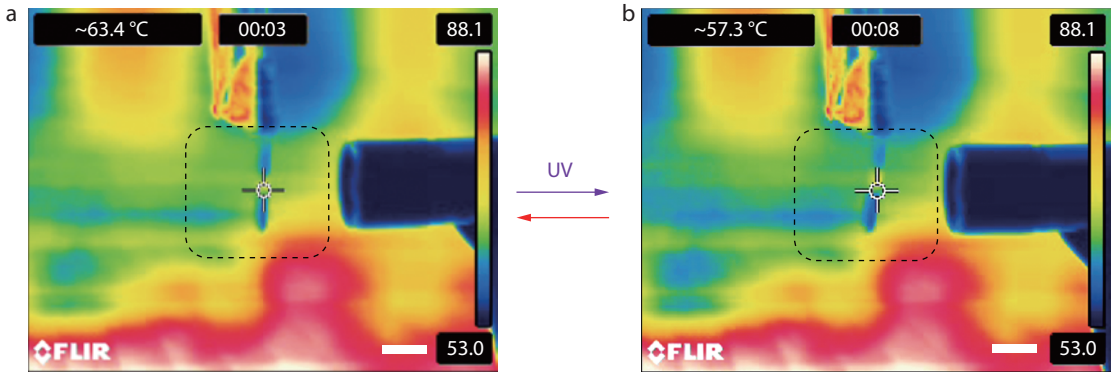

Fig. 6 The infrared imageries of the reversible photo-induced deformation of PC11AE6 films at about 60 °C. (a) The initial state of films at about 60 °C in oven. (b) The bending of films under UV irradiation from right to left. The UV light intensity was always kept at 40 mW·cm^{-2}. The size of films used here is 5 mm × 1 mm × 10 μm. The scale bar is 2 mm. The transient temperatures of films marked by a white cross were recorded and showed in the upper left corner of imageries.

https://doi.org/10.1007/s10118-020-2383-0

from one side.[34] The resistance existing intrinsically in the thicker film was larger than that of the thinner one, which brought small bending angle under the same irradiation condition. However, fibre with a diameter of 40 μm exhibited better photoresponsibility compared with film with a diameter of 10 μm under the same irradiation condition because of the increased order parameter (Movie S3 in ESI). Besides, as shown in Fig. 5(b) and Fig. S6 (in ESI), with UV light intensity increasing, films and fibres showed larger bending angles, which was caused by the more *trans-cis* photoisomerization driven by high photon energy. The average angular speed was used to quantify the photodeformation velocity. An average angle speed of 1.25 (°)·s^{-1} was achieved for film and 3.67 (°)·s^{-1} was reached for fibre under the same irradiation. After visible light irradiation with constant intensity (50 mW·cm^{-2}), the bent PC11AE6 films and fibres recovered in 30 s, indicating that the deformation of PC11AE6 films was completely reversible.

The PC11AE6 film was used to investigate the photoinduced deformation of PC11AE6 at an elevated temperature, as shown in Fig. 6. When the temperature was around 60 °C, which was in the temperature range of smectic A phase, film bent away from the light source in 5 s under UV irradiation, and then it recovered immediately after removing the UV light (Movie S4 in ESI). This spontaneously recovering phenomenone may be caused by the on-going *cis-trans* back isomerization which was accelerated by heating because of the thermodynamic instability of *cis* form.

CONCLUSIONS

We designed an azoester-containing linear liquid crystal polymer PC11AE6 with excellent mesophase stability and photoresponsibility. The polymer exhibited wide mesophase temperature range, which possessed two mesophases in the process of heating or cooling and a high isotropic temperature (182 °C). Thanks to the spontaneous orientation ability of polymer, PC11AE6 films and fibres possessed anisotropic structures with smectic A phase at room temperature and smectic C phase at elevated temperatures. With out-of-plane orientation of mesogens, the PC11AE6 films bent away from the UV source and unbent completely under visible light irradiation. The effects of UV light intensity and the film thickness on the photodeformation of PC11AE6 were investigated. The bending angle increased with the UV light intensity increasing, and was larger for the thinner film than that of the thicker one. The maximum bending angle of free-standing films was 68° for 10 μm thickness with an average angle speed of 1.25 (°)·s^{-1} under UV irradiation (40 mW·cm^{-2}). Owing to higher orientation parameter compared with films, a rapid and reversible deformation was obtained by PC11AE6 fibres under the same irradiation with an average angle speed of 3.67 (°)·s^{-1}. Furthermore, the free-standing film still possessed photoresponsibility under UV irradiation at about 60 °C. These results provide insight into the design of a LLCP with broad mesophase temperature range to satisfy different demands for applications.

Electronic Supplementary Information

Electronic supplementary information (ESI) is available free of charge in the online version of this article at http://dx.doi.org/10.1007/s10118-020-2383-0.

ACKNOWLEDGMENTS

This work was financially supported by the National Natural Science Foundation of China (Nos. 21734003, 51573029, and 51721002), Natural Science Foundation of Shanghai (No. 17ZR1440100), and Innovation Program of Shanghai Municipal Education Commission (No. 2017-01-07-00-07-E00027).

REFERENCES

1 Liao, J.; Yang, M.; Liu, Z.; Zhang, H. Fast photoinduced deformation of hydrogen-bonded supramolecular polymers containing α-cyanostilbene derivative. *J. Mater. Chem. A* **2019**, *7*, 2002–2008.
2 Yu, Y.; Ikeda, T. Photodeformable polymers: a new kind of promising smart material for micro- and nano-applications. *Macromol. Chem. Phys.* **2005**, *206*, 1705–1708.
3 Gelebart, A. H.; Mulder, D. J.; Varga, M.; Konya, A.; Vantomme, G.; Meijer, E. W.; Selinger, R. L. B.; Broer, D. J. Making waves in a photoactive polymer film. *Nature* **2017**, *546*, 632.
4 Iamsaard, S.; Asshoff, S. J.; Matt, B.; Kudernac, T.; Cornelissen, J. J. L. M.; Fletcher, S. P.; Katsonis, N. Conversion of light into macroscopic helical motion. *Nat. Chem.* **2014**, *6*, 229–235.
5 Yamada, M.; Kondo, M.; Miyasato, R.; Naka, Y.; Mamiya, J.; Kinoshita, M.; Shishido, A.; Yu, Y.; Barrett, C. J.; Ikeda, T. Photomobile polymer materials-various three-dimensional movements. *J. Mater. Chem.* **2009**, *19*, 60–62.
6 Yu, Q.; Yang, X.; Chen, Y.; Yu, K.; Gao, J.; Liu, Z.; Cheng, P.; Zhang, Z.; Aguila, B.; Ma, S. Fabrication of light-triggered soft artificial muscles *via* a mixed-matrix membrane strategy. *Angew. Chem. Int. Ed.* **2018**, *57*, 10192–10196.
7 Li, Y.; Rios, O.; Keum, J. K.; Chen, J.; Kessler, M. R. Photoresponsive liquid crystalline epoxy networks with shape memory behavior and dynamic ester bonds. *ACS Appl. Mater. Interfaces* **2016**, *8*, 15750–15757.
8 Wei, J.; Yu, Y. Photodeformable polymer gels and crosslinked liquid-crystalline polymers. *Soft Matter* **2012**, *8*, 8050–8059.
9 Yu, H.; Tang, J.; Feng, Y.; Feng, W. Structural design and application of azo-based supramolecular polymer systems. *Chinese J. Polym. Sci.* **2019**, *37*, 1183–1199.
10 Liu, Q.; Liu, Y.; Lv, J.; Chen, E.; Yu, Y. Photocontrolled liquid transportation in microtubes by manipulating mesogen orientations in liquid crystal polymers. *Adv. Intell. Syst.* **2019**, *1*, 1900060.
11 Lv, J.; Liu, Y.; Wei, J.; Chen, E.; Qin, L.; Yu, Y. Photocontrol of fluid slugs in liquid crystal polymer microactuators. *Nature* **2016**, *537*, 179.
12 Xu, B.; Zhu, C.; Qin, L.; Wei, J.; Yu, Y. Light-directed liquid manipulation in flexible bilayer microtubes. *Small* **2019**, *15*, 1901847.
13 Finkelmann, H.; Kim, S. T.; Munoz, A.; Palffy-Muhoray, P.; Taheri, B. Tunable mirrorless lasing in cholesteric liquid crystalline elastomers. *Adv. Mater.* **2001**, *13*, 1069.
14 Kumar, K.; Knie, C.; Bleger, D.; Peletier, M. A.; Friedrich, H.; Hecht, S.; Broer, D. J.; Debije, M. G.; Schenning, A. P. H. J. A chaotic self-oscillating sunlight-driven polymer actuator. *Nat. Commun.* **2016**, *7*, 11975.
15 Urayama, K.; Arai, Y. O.; Takigawa, T. Volume phase transition of monodomain nematic polymer networks in isotropic solvents accompanied by anisotropic shape variation. *Macromolecules*

2005, *38*, 3469–3474.
16 Gebhard, E.; Zentel, R. Ferroelectric liquid crystalline elastomers 2. Variation of mesogens and network density. *Macromol. Chem. Phys.* **2000**, *201*, 911–922.
17 Buguin, A.; Li, M. H.; Silberzan, P.; Ladoux, B.; Keller, P. Micro-actuators: when artificial muscles made of nematic liquid crystal elastomers meet soft lithography. *J. Am. Chem. Soc.* **2006**, *128*, 1088–1089.
18 Yang, Z.; Herd, G. A.; Clarke, S. M.; Tajbakhsh, A. R.; Terentjev, E. M.; Huck, W. T. S. Thermal and UV shape shifting of surface topography. *J. Am. Chem. Soc.* **2006**, *128*, 1074–1075.
19 Pang, X.; Lv, J.; Zhu, C.; Qin, L.; Yu, Y. Photodeformable azobenzene-containing liquid crystal polymers and soft actuators. *Adv. Mater.* **2019**, *31*, 1904224.
20 Weis, P.; Wu, S. Light-switchable azobenzene-containing macromolecules: from UV to near infrared. *Macromol. Rapid Commun.* **2018**, *39*, 1700220.
21 Li, X.; Fang, L.; Hou, L.; Zhu, L.; Zhang, Y.; Zhang, B.; Zhang, H. Photoresponsive side-chain liquid crystalline polymers with amide group-substituted azobenzene mesogens: effects of hydrogen bonding, flexible spacers, and terminal tails. *Soft Matter* **2012**, *8*, 5532–5542.
22 Jadeja, U. H.; Sharma, V. S.; Prajapat, V.; Shah, A.; Sharma, A. S. Synthesis and study of azo based liquid crystals: effect of the lateral bromo and terminal alkoxy side chain on thermal, mesomorphic and optical properties. *Mol. Cryst. Liq. Cryst.* **2019**, *680*, 46–64.
23 Jadeja, U. H.; Patel, R. B. The effect of molecular rigidity and flexibility on the mesomorphism of azoesters. *Mol. Cryst. Liq. Cryst.* **2016**, *637*, 28–36.
24 Okano, K.; Tsutsumi, O.; Shishido, A.; Ikeda, T. Azotolane liquid-crystalline polymers: huge change in birefringence by photoinduced alignment change. *J. Am. Chem. Soc.* **2006**, *128*, 15368–15369.
25 Zhang, L.; Yao, W.; Gao, Y.; Zhang, C.; Yang, H. Polysiloxane-based side chain liquid crystal polymers: from synthesis to structure-phase transition behavior relationships. *Polymers* **2018**, *10*, 794.
26 Yin, R.; Xu, W.; Kondo, M.; Yen, C.; Mamiya, J.; Ikeda, T.; Yu, Y. Can sunlight drive the photoinduced bending of polymer films? *J. Mater. Chem.* **2009**, *19*, 3141–3143.
27 Breitenkamp, K.; Simeone, J.; Jin, E.; Emrick, T. Novel amphiphilic graft copolymers prepared by ring-opening metathesis polymerization of poly(ethylene glycol)-substituted cyclooctene macromonomers. *Macromolecules* **2002**, *35*, 9249–9252.
28 Li, X.; Wen, R.; Zhang, Y.; Zhu, L.; Zhang, B.; Zhang, H. Photoresponsive side-chain liquid crystalline polymers with an easily cross-linkable azobenzene mesogen. *J. Mater. Chem.* **2009**, *19*, 236–245.
29 Pang, X.; Xu, B.; Qing, X.; Wei, J.; Yu, Y. Photo-induced bending behavior of post-crosslinked liquid crystalline polymer/polyurethane blend films. *Macromol. Rapid Commun.* **2018**, *39*, 1700237.
30 De-Haan, L. T.; Gimenez-Pinto, V.; Konya, A.; Thanh-Son, N.; Verjans, J. M. N.; Sanchez-Somolinos, C.; Selinger, J. V.; Selinger, R. L. B.; Broer, D. J.; Schenning, A. P. H. J. Accordion-like actuators of multiple 3D patterned liquid crystal polymer films. *Adv. Funct. Mater.* **2014**, *24*, 1251–1258.
31 Liu, Q.; Zhan, Y.; Wei, J.; Ji, W.; Hu, W.; Yu, Y. Dual-responsive deformation of a crosslinked liquid crystal polymer film with complex molecular alignment. *Soft Matter* **2017**, *13*, 6145–6151.
32 Xia, Y.; Cedillo-Servin, G.; Kamien, R. D.; Yang, S. Guided folding of nematic liquid crystal elastomer sheets into 3D *via* patterned 1D microchannels. *Adv. Mater.* **2016**, *28*, 9637.
33 Kondo, M.; Yu, Y.; Ikeda, T. How does the initial alignment of mesogens affect the photoinduced bending behavior of liquid-crystalline elastomers? *Angew. Chem. Int. Ed.* **2006**, *45*, 1378–1382.
34 Wang, Z.; Zhang, H. Synthesis of an azobenzene-containing main-chain crystalline polymer and photodeformation behaviors of its supramolecular hydrogen-bonded fibers. *Chinese J. Polym. Sci.* **2020**, *38*, 37–44.

https://doi.org/10.1007/s10118-020-2383-0